ANATOMICAL PATHOLOGY

Appl1, Sortilin and Syndecan-1 immunohistochemistry on intraductal carcinoma of the prostate provides evidence of retrograde spread

ALEXANDRA SORVINA[1,*], CARMELA MARTINI[1,*], SARITA PRABHAKARAN[1,2,*], JESSICA M. LOGAN[1,*], BENJAMIN S-Y. UNG[1], COURTNEY MOORE[1], IAN R. D. JOHNSON[1], JOANNA LAZNIEWSKA[1], PRERNA TEWARI[3], VICTORIA MALONE[4], ROBERT D. BROOKS[1], SHANE M. HICKEY[1], MARIA C. CARUSO[1], SONJA KLEBE[2,5], LITSA KARAGEORGOS[1], JOHN J. O'LEARY[3], BRETT DELAHUNT[6], HEMAMALI SAMARATUNGA[7,8,†], DOUG A. BROOKS[1,†]

[1]Clinical and Health Sciences, University of South Australia, Adelaide, SA, Australia; [2]Department of Anatomical Pathology, College of Medicine and Public Health, Flinders University, Adelaide, SA, Australia; [3]Department of Histopathology, Trinity College Dublin, Dublin, Ireland; [4]Department of Pathology, The Coombe Women and Infants University Hospital, Dublin, Ireland; [5]Department of Surgical Pathology, SA Pathology at Flinders Medical Centre, Adelaide, SA, Australia; [6]Malaghan Institute of Medical Research, Wellington, New Zealand; [7]Aquesta Uropathology, Brisbane, Qld, Australia; [8]University of Queensland, Brisbane, Qld, Australia; [*]equal first authors; [†]equal last authors

Summary

The presence of intraductal carcinoma of the prostate (IDCP) correlates with late-stage disease and poor outcomes for patients with prostatic adenocarcinoma, but the accurate and reliable staging of disease severity remains challenging. Immunohistochemistry (IHC) has been utilised to overcome problems in assessing IDCP morphology, but the current markers have only demonstrated limited utility in characterising the complex biology of this lesion. In a retrospective study of a cohort of patients who had been diagnosed with IDCP, we utilised IHC on radical prostatectomy sections with a biomarker panel of Appl1, Sortilin and Syndecan-1, to interpret different architectural patterns and to explore the theory that IDCP occurs from retrograde spread of high-grade invasive prostatic adenocarcinoma. Cribriform IDCP displayed strong Appl1, Sortilin and Syndecan-1 labelling patterns, while solid IDCP architecture had high intensity Appl1 and Syndecan-1 labelling, but minimal Sortilin labelling. Notably, the expression pattern of the biomarker panel in regions of IDCP was similar to that of adjacent invasive prostatic adenocarcinoma, and also comparable to prostate cancer showing perineural and vascular invasion. The Appl1, Sortilin, and Syndecan-1 biomarker panel in IDCP provides evidence for the model of retrograde spread of invasive prostatic carcinoma into ducts/acini, and supports the inclusion of IDCP into the five-tier Gleason grading system.

INTRODUCTION

Prostate cancer is the second most common cancer in men worldwide, involving the diagnosis of over 1.4 million patients and resulting in more than 375,000 deaths annually.[1] While the incidence of intraductal carcinoma of the prostate (IDCP) varies between different studies,[2–4] there is common agreement that the presence of an IDCP component within a prostate tissue sample correlates with high-stage disease and a poorer prognosis.[5,6] However, the reporting of IDCP remains subjective and suffers from conflicting criteria and definitions.[7–9] In particular, the International Society of Urological Pathology (ISUP) recommends incorporating IDCP into the five-tier Gleason grading system, when it is found in association with invasive carcinoma.[8] Conversely, the Genitourinary Pathology Society (GUPS) suggests the reporting of IDCP as an explanatory comment, independent of Gleason grading.[7,8] These conflicting recommendations create confusion in the reporting of IDCP, with downstream problems comparing different studies or standardising patient management.

Controversies relating to IDCP reporting stem from the proposal that IDCP is a biological entity distinct from invasive prostate adenocarcinoma, as reported in 2016 by the World Health Organization (WHO) classification of tumours of the prostate gland.[10] This has led to the creation of inconsistent strategies that attempt to define the nature of IDCP more accurately. Morphologically, IDCP is characterised by the presence of a lumen-spanning proliferation of neoplastic epithelium within pre-existing prostatic ducts and acini, with retention of basal cells.[11] IDCP shares similar morphological features to other lesions in the prostate including high-grade prostatic intraepithelial neoplasia, cribriform acinar adenocarcinoma, ductal adenocarcinoma, and intraductal spread of urothelial carcinoma.[12] These key features which are indicative

of, but not unique to IDCP, include intraductal and intra-acinar growth of cancer cells with cribriform and solid patterns, marked nuclear atypia/enlargement and comedonecrosis.[10,12–14] Transcriptional regulator ERG expression and phosphatase and tensin homolog (PTEN) loss were initially utilised to define a diagnostic profile for IDCP. However, the ERG/PTEN status of invasive prostatic adenocarcinoma and areas of atypical proliferation share a similarity to IDCP in >90% of cases.[15–17] This is not surprising if IDCP is considered to represent retrograde colonisation of the prostatic ducts and acini by invasive high-grade prostatic adenocarcinoma, with several lines of evidence supporting a theory that IDCP represents intra-acinar and intraductal invasion of pre-existing invasive carcinoma, rather than a *de novo* precancerous lesion.[18,19] Both Gleason grading and the diagnosis of IDCP rely on the assessment of morphological criteria. Currently, the lack of effective biomarkers that define the underlying cell biology of the disease has limited the field's capacity to resolve these controversies and implement an appropriate approach to tumour grading.

We recently reported results from a set of biomarkers that define the primary pathology of prostate cancer in patient tissue and can predict patient outcome.[20–24] Appl1, Sortilin and Syndecan-1 are key endosomal proteins and have regulatory roles in respectively transcription factor activity, energy metabolism and cancer progression.[25–27] Appl1, localised to early endosomes, regulates vesicle transport by controlling the speed of cargo internalisation. Sortilin controls the biogenesis of GLUT transporter vesicles and transport from the trans-Golgi network to endosomes, lysosomes, secretory granules and the plasma membrane.[28] Syndecan-1 is a heparan sulphate proteoglycan involved in cell proliferation, migration and cell-matrix interactions. The combined assessment of Appl1, Sortilin and Syndecan-1 protein expression by IHC improved the reliability of prostate cancer assessment and more accurately interpreted the morphologies that represent the transition between low-grade and high-grade disease. Here, we have used this novel panel of biomarkers to evaluate a retrospective series of prostate cancer patients with confirmed IDCP, to further characterise the complex biology between these two lesions and reveal that these biomarkers have the potential to resolve some of the problems arising from a purely morphological approach to IDCP interpretation.

MATERIALS AND METHODS

Patient samples and ethical approval

Prostate tissue specimens were obtained from 100 patients with prostate cancer, who had been treated by radical prostatectomy and had confirmed presence of IDCP. Tissue samples were accessioned within the period of December 2019 to February 2020 by Aquesta Uropathology, Brisbane, Australia.[29] Prior to surgery, all patients were treatment naïve,[29] and cases were diagnosed by a specialist uropathologist utilising the criteria of the 2005 modified Gleason grading system and the recommendations of the 2014 International Society of Urological Pathology Consensus Conference.[13,29,30]

Ethics approval for sample access and use of de-identified human prostate tissues was obtained through the institutional review board, Human Research Ethics Committee of the University of South Australia (Application IDs: 201907 and 0000036070), and Aquesta Uropathology (Application ID: 2020–003). All experiments were performed in accordance with the guidelines of the National Statement on Ethical Conduct in Human Research and National Health and Medical Research Council of Australia.

Histopathology and immunohistochemistry on IDCP cases

Tissue sections, representative of the prostate cancer in each case, were identified by a specialist uropathologist (HS) and further sections were cut at 4

µm thickness from the formalin-fixed, paraffin-embedded (FFPE) blocks held by Aquesta Uropathology, Brisbane, Australia. For each case, the highest grade tumour block was selected for the study. Sections were mounted on Superfrost Ultra Plus slides (Menzel–Gläser, Germany) and heated at 60°C for 1 h before storage at 4°C. Tissue sections were stained with routine Ehrlich's haematoxylin and eosin (H&E; Australian Biostain, Australia),[31] using the Leica ST5010 Autostainer XL (Leica Biosystems, Australia) automated staining platform.

Immunohistochemical labelling of the biomarker panel (Appl1, Sortilin, and Syndecan-1), and the basal cell cocktail (34βE12+p63; Roche, Australia) with prostate P504S marker (Roche) was performed on a Ventana BenchMark Ultra platform (Roche Diagnostics, Australia). Briefly, epitope retrieval was performed in CC1 buffer (at 95°C for 32 min for the biomarker panel, and 64 min for the 34βE12+P63/P504S; Roche). Tissue sections were then incubated with monoclonal antibodies to Appl1, Sortilin or Syndecan-1,[20] for 1 h at 36°C, or with 34βE12+P63 for 32 min and P504S for 16 min at 36°C. Detection and visualisation were performed using the OptiView DAB Detection Kit (Roche). Tissue sections were counterstained with Gill's haematoxylin (Roche) and mounted with DPX mounting medium (Thermo-Fisher Scientific, Australia). All tissue slides were scanned using a Zeiss Axio Scan.Z1 in brightfield mode, with a Plan-Achromat 20× objective (Zeiss, Germany), and images collated in Adobe Photoshop 2020 (Adobe Systems, USA).

RESULTS

Characterisation of IDCP in tissue samples from patients with prostate cancer

Of the 100 patient samples recruited for the study, three cases were excluded due to technical issues during tissue immunolabelling. All cases were identified to have adjacent invasive acinar carcinoma and confirmation of IDCP was achieved by H&E and IHC assessment (34βE12+P63/P504S), using the morphological criteria of the 2016 edition of the WHO Classification of Tumours of the Prostate Gland.[10,12] Assessment by standard practice enabled the identification of different architectural patterns of IDCP, including loose and dense cribriform IDCP, solid IDCP, and IDCP with comedonecrosis (Fig. 1). In cases demonstrating cribriform pattern structures, the possibility of an atypical proliferation suspicious for intraductal carcinoma (ASID) was ruled out due to the presence of malignant nuclear features. High-power images of the cribriform examples shown in Fig. 1 demonstrate cytological atypia (Supplementary Fig. 1, Appendix A) in cases of loose and dense cribriform IDCP. The 34βE12+P63/P504S IHC labelling identified scattered cancer cells (P504S positive) and a complete (loose cribriform) or incomplete (dense, solid and comedonecrosis IDCP) basal cell layer (34βE12+P63). Most cases exhibited variable immunoreactivity for 34βE12+P63/P504S throughout the regions of tissue with IDCP. While several architectural patterns were often present in the same tissue section, the cribriform IDCP pattern was the most prominent, followed by solid IDCP (Supplementary Table 1, Appendix A).

Expression of Appl1, Sortilin and Syndecan-1 is indicative of the biological significance of the architectural patterns of IDCP

Appl1 labelling in cancer cells within regions of IDCP was strong and diffuse, and mapped the architecture of the cancer (Fig. 2, first and second column); Sortilin labelling was punctate and varied in intensity between different architectural patterns (Fig. 2, third column); and Syndecan-1 strongly labelled the cancer cells in all IDCP patterns. Syndecan-1
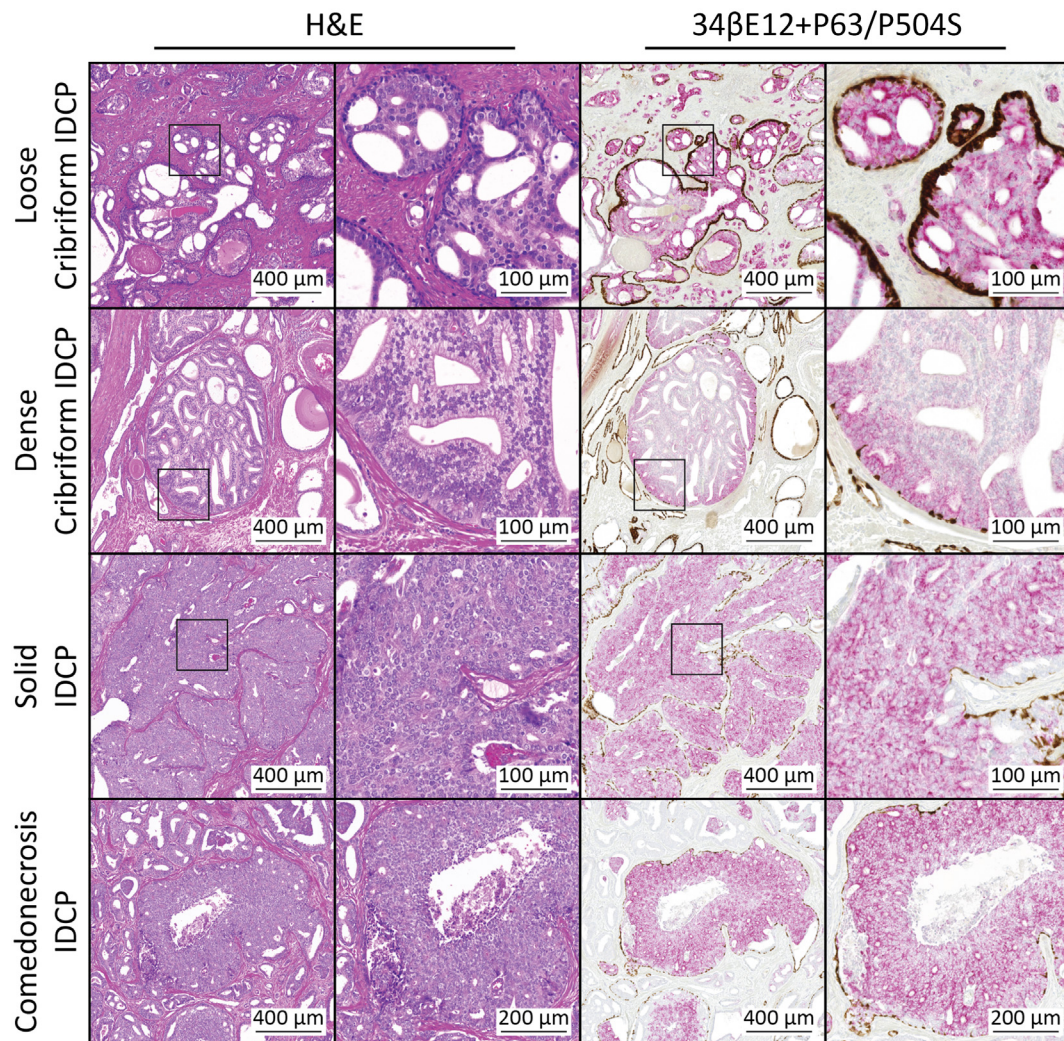
Fig. 1 Architectural patterns of intraductal carcinoma of the prostate (IDCP). Representative images of architectural patterns of IDCP including loose and dense cribriform, solid IDCP and comedonecrosis IDCP. Patterns were visualised on H&E-stained prostate tissue sections (first column and magnified in second column) with corresponding images showing immunoreactivity for 34βE12+P63/P504S (third column and magnified in fourth column). Nuclei were stained with Ehrlich's haematoxylin (H&E) and Gill's haematoxylin (IHC).

labelling was particularly evident in peripheral regions of the ducts involved, albeit with lower labelling intensity in the central regions of the cancer (Fig. 2, fourth column). This pattern of Syndecan-1, IDCP was confirmed in 73 of 97 cases (75%).

A qualitative assessment of the intensity of labelling of Appl1/Sortilin/Syndecan-1 according to the different IDCP patterns was also conducted. Appl1 consistently displayed a high expression level in cribriform IDCP, solid IDCP and IDCP with comedonecrosis (89–92% samples). Not surprisingly, Sortilin demonstrated low expression levels, with only up to 46% of cases displaying moderate expression but the expression was never high. Syndecan-1 had moderate expression in most cases (93–97%). While there was loss of a polarised distribution pattern for Sortilin in cribriform IDCP (Fig. 2), this was not always reflected in the intensity values.

When considered in combination, Appl1 and Syndecan-1 showed strong immunolabelling in cribriform IDCP patterns, and Sortilin exhibited polarised labelling that was evident in both loose and dense cribriform IDCP patterns (Fig. 2, top rows), similar to the pattern of expression in Gleason pattern 3 glands (Supplementary Fig. 2, Appendix

A). Appl1 and Syndecan-1 also showed strong immunolabelling in solid and IDCP with comedonecrosis, but Sortilin immunolabelling was either absent or disseminated in these tissue patterns (Fig. 2, bottom rows), similar to the pattern of expression in higher grade patterns of cancer (pattern 4 glands, Supplementary Fig. 2, Appendix A). Sortilin loss or minimal immunolabelling in cancer tissue combined with strong Appl1 and Syndecan-1 immunolabelling was observed, as we have previously demonstrated in high-grade prostate cancer.[20] Here, the punctate expression pattern for Sortilin with a polarised supranuclear location, combined with strong Appl1 and Syndecan-1 labelling, suggested that the cribriform IDCP patterns had a less aggressive phenotype than solid or comedonecrosis IDCP patterns (Fig. 2, see also direct comparison in Supplementary Fig. 3, Appendix A).

Characterisation of IDCP and adjacent invasive prostatic adenocarcinoma using Appl1, Sortilin and Syndecan-1 IHC biomarker labelling

To further explore the theory that IDCP represents a retrograde spread of invasive high-grade prostatic adenocarcinoma, the
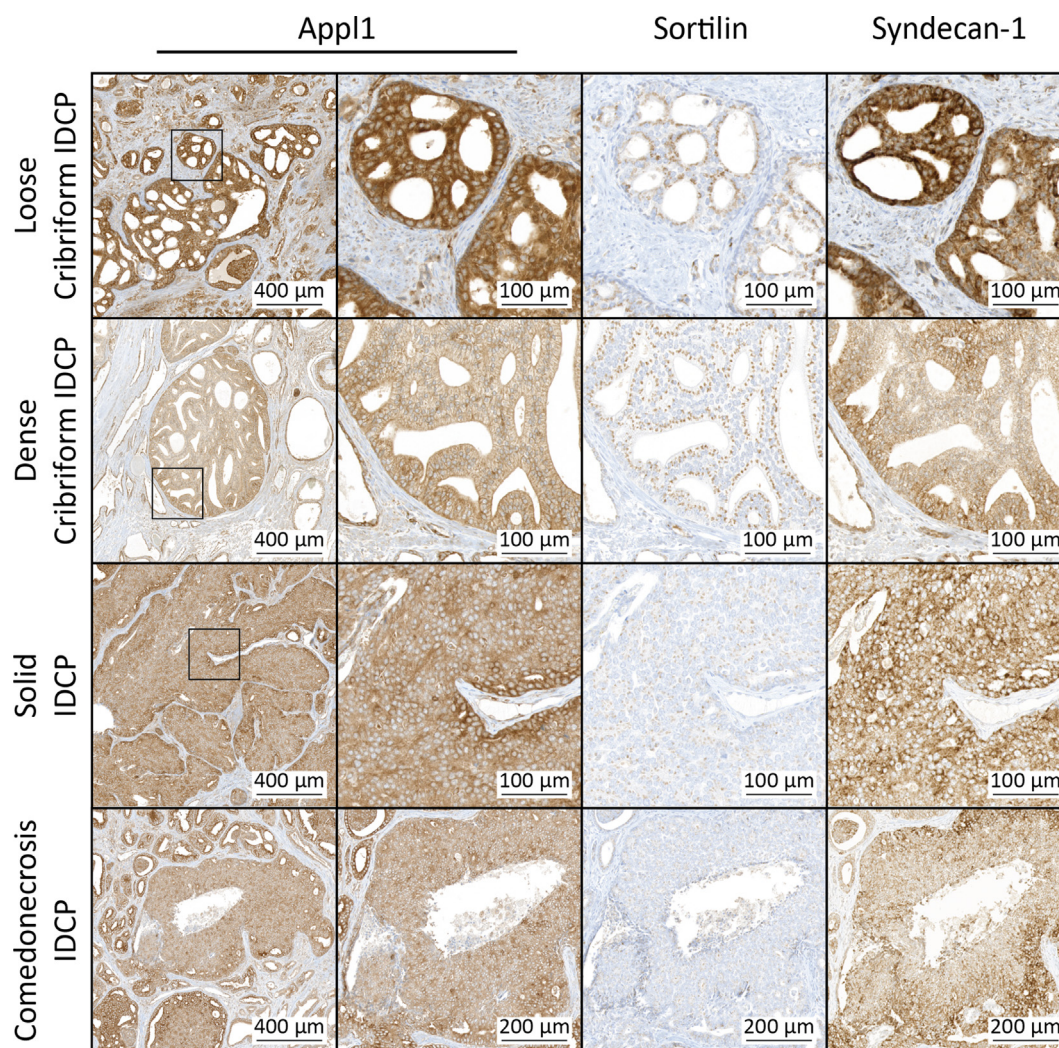
Fig. 2 Appl1, Sortilin and Syndecan-1 expression in architectural patterns of intraductal carcinoma of the prostate (IDCP). Representative images of architectural patterns of IDCP including loose and dense cribriform, solid IDCP and comedonecrosis IDCP. Patterns of IDCP were visualised on prostate tissue sections immunolabelled with antibodies against Appl1 (first column and magnified in second column), Sortilin (third column) and Syndecan-1 (fourth column). Nuclei were stained with Gill's haematoxylin (IHC).

biomarker panel was used to investigate regions of invasive adenocarcinoma adjacent to IDCP foci. IDCP and adjacent invasive high-grade cancer glands showed similar patterns of Appl1, Sortilin and Syndecan-1 immunolabelling, consistent with a similar grade of cancer, suggestive of a common origin (Fig. 3). For example, when Sortilin immunolabelling was detected with strong Appl1 and Syndecan-1 immunolabelling in IDCP, the adjacent invasive glands had an identical pattern of biomarker labelling (Fig. 3, top row). Similarly, in cases with low Sortilin labelling intensity and strong Appl1 and Syndecan-1 expression in IDCP, the adjacent invasive prostatic adenocarcinoma displayed the same pattern of biomarker labelling (Fig. 3, bottom row). This matched pattern of biomarker labelling between IDCP and the adjacent invasive prostatic adenocarcinoma was confirmed in 61 of 73 cases (84%).

Additional pathological features consistent with the retrograde spread of the invasive cancer were also present in the tissue samples from patients with IDCP. Perineural invasion was identified in all cases, and vascular invasion was also commonly observed (see examples in Fig. 4). The series of cases also displayed evidence of partial ductal involvement, providing visual evidence of the ductal invasion process (Fig. 4, bottom row). These data reveal that the biomarker panel effectively identifies invasive high-grade cancer cells and provides evidence that the invasive adenocarcinoma and the cancer cells being disseminated into prostatic ducts (IDCP) have a common phenotype, indicative of retrograde spread.

DISCUSSION

IDCP reporting can be challenging because of the morphological overlap with invasive cribriform prostatic adenocarcinoma, urothelial carcinoma extending into prostatic ducts and prostatic ductal carcinoma, which each share a variety of malignant cytological features on H&E-stained tissue.[13,14] Current markers such as 34βE12, high molecular weight cytokeratins and the P63/P504S cocktail[32,33] have provided only limited clinical utility for characterising and interpreting the complex biology of these lesions. IDCP most probably represents a retrograde colonisation of the prostatic ducts and acini by invasive high-grade prostatic adenocarcinoma, with several lines of evidence supporting this theory.[18,19] In this
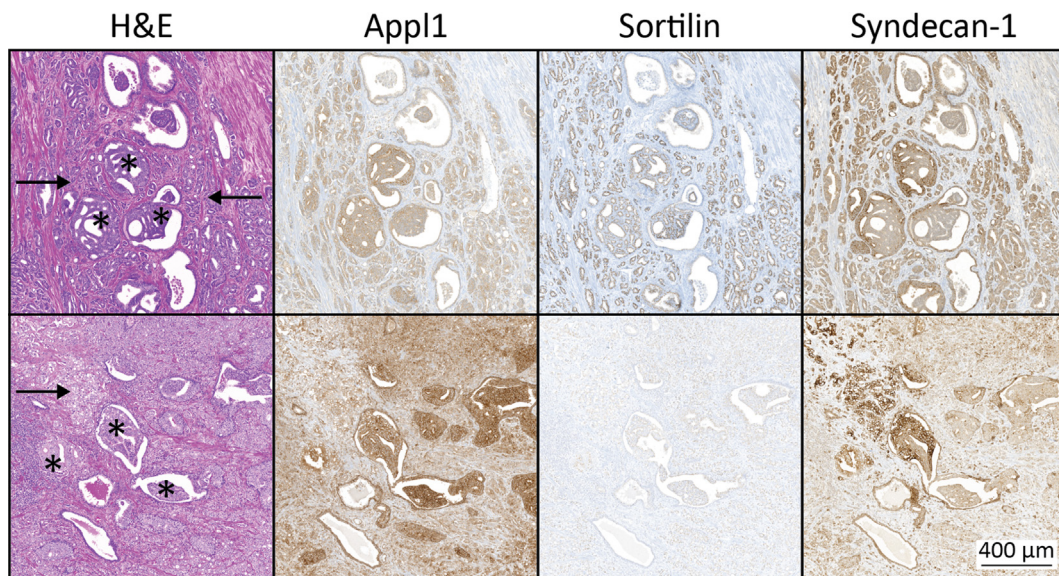
Fig. 3 Biomarker labelling pattern in invasive high-grade prostatic adenocarcinoma regions adjacent to intraductal carcinoma of the prostate (IDCP). Representative examples of foci of invasive prostatic adenocarcinoma (arrows) adjacent to IDCP regions (stars) were stained by H&E (first column) and immunolabelled with antibodies against Appl1 (second column), Sortilin (third column) and Syndecan-1 (fourth column). Nuclei were stained with Ehrlich's haematoxylin (H&E) and Gill's haematoxylin (IHC).
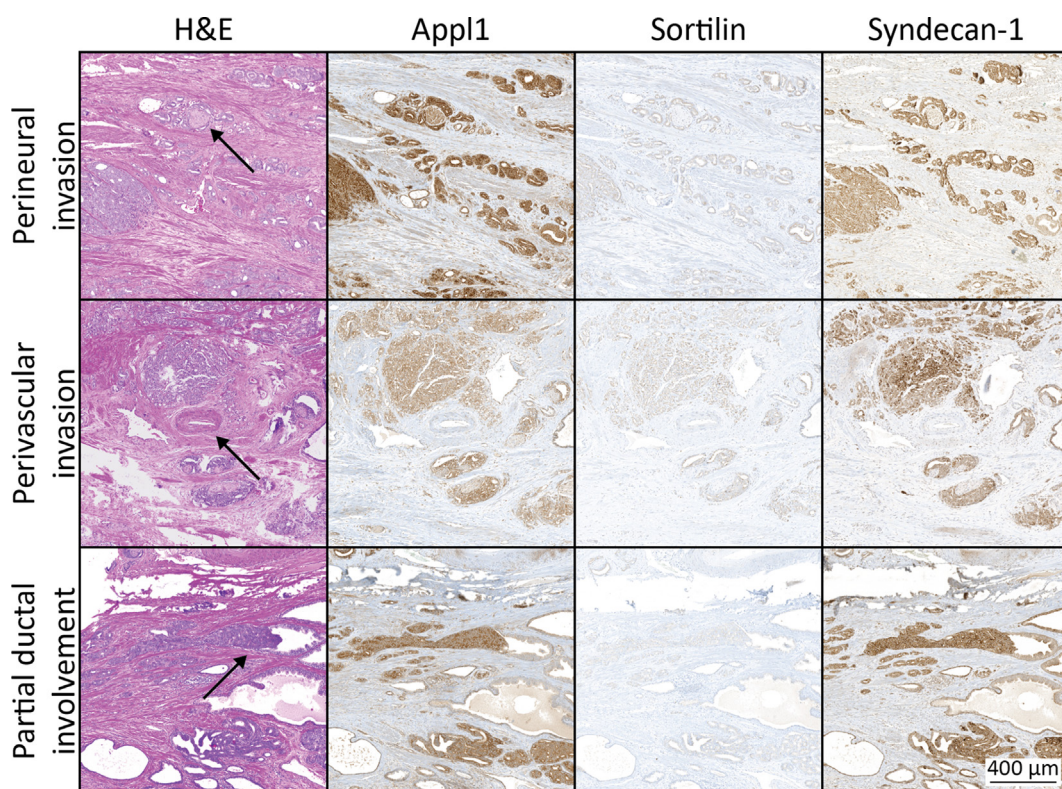

Fig. 4 Retrograde spread of invasive high-grade prostatic adenocarcinoma. Representative examples of retrograde spread of invasive prostatic adenocarcinoma, including perineural invasion (top row, arrow indicating nerve bundle), perivascular involvement (middle row, arrow indicating blood vessel) and partial ductal involvement (bottom row, arrow indicating cancer cells partially occluding duct) were stained with H&E (first column) and immunolabelled with antibodies against Appl1 (second column), Sortilin (third column) and Syndecan-1 (fourth column). Nuclei were stained with Ehrlich's haematoxylin (H&E) and Gill's haematoxylin (IHC).

current study, we utilised the biomarker panel of Appl1, Sortilin and Syndecan-1 by IHC[20] to characterise IDCP and compare labelling patterns in IDCP to that of adjacent invasive prostatic adenocarcinoma.

Appl1, Sortilin and Syndecan-1 have important functions in the endosome-lysosome system, and these biomarkers correlate with critical points of pathogenesis in prostate cancer.[20,23] Appl1, is a multifunctional endocytic adaptor

protein that also has a role as a transcription factor,[34] and using IHC on prostate cancer tissue sections accurately maps the cancer and can discriminate benign glands.[20,23] Sortilin mediates the transport of specific intracellular cargo from the trans-Golgi network to the plasma membrane and endosomes, and it is integrally involved in GLUT4-mediated sugar metabolism.[35,36] It is highly expressed in metabolically active tissues and cells, and it is indicative of low-grade prostate cancer tissue.[20] Syndecan-1 mediates growth factor binding and cell migration and is highly expressed in advanced cancer morphologies including poorly formed glands, nests, cords of cells, cribriform and IDCP.[20] The combined analysis of this panel of biomarkers has been used to accurately map the pathogenesis in prostate cancer tissue,[20] and is currently being evaluated for its capacity to predict clinical outcomes.

In the current study, Appl1, Sortilin and Syndecan-1 IHC identified regions of IDCP and invasive prostatic adenocarcinoma in tissues from patients with prostate cancer. In IDCP, Appl1 labelling accurately depicts the cancer architecture, while Sortilin displays predominantly a low-to-moderate labelling pattern of expression, similar to previous observations in prostatic adenocarcinoma.[20] Syndecan-1 displays intense peripheral labelling of IDCP, with low labelling intensity in central areas of the involved ducts and acini. The variable intensity of Syndecan-1 immunolabelling suggests that IDCP is metabolically heterogeneous, which can promote cell migratory potential in response to hypoxic conditions in the core regions of IDCP. This biphenotypic expression of peripheral versus central cancer cell populations has also been observed in cribriform patterns of prostate cancer labelled for PTEN and P27 loss, and CD44 variant 7/8 expression.[37] Moreover, we commonly observed a reduction of Syndecan-1 levels in core regions of IDCP, known to occur in response to hypoxia,[38] which may be consistent with necrosis and unfavourable patient outcomes.[39–41] Furthermore, both IDCP and cribriform prostatic adenocarcinoma have been associated with hypoxia[41] and have similarities in their biological significance.[11]

The effects of hypoxia on Sortilin in prostate cancer and IDCP are yet to be elucidated; however, studies conducted in the central nervous system have found that hypoxia and several other stressors including acidosis, oxidative stress, and glucose deprivation induce progranulin expression (a secreted growth factor and ligand for Sortilin).[42,43] As progranulin binding to Sortilin impairs the protective effects of progranulin and progranulin-mediated signalling, protection against stressors is sustained through the degradation of Sortilin.[44,45] In the context of prostate cancer, the relationship between Sortilin and progranulin is more complicated, with evidence suggesting that IDCP represents a hypoxic environment, comprised of androgen-insensitive cells.[38,46,47] Interestingly, in androgen-insensitive cells, progranulin can induce Sortilin degradation to maintain small amounts of the receptor and high progranulin levels, consequently promoting prostate cancer progression (cancer cell motility, invasion, and anchorage-independent growth).[27,44,48] In addition, the hypoxic environment present in IDCP, presumably arising as the cells have minimal contact with the vascularised stromal environment,[39,47] may exacerbate the Sortilin/progranulin axis in a similar manner to the central nervous

system's response against stressors. Indeed, it is well established that the prostate and the brain are known to display similar endosomal trafficking pathways.[49] We noted that Sortilin is mainly expressed at low-to-moderate levels in IDCP, presumably in result of degradation induced by progranulin (whether through hypoxic conditions or the androgen-insensitive properties of IDCP cancer cells). The idea that progranulin maintains low levels of Sortilin in IDCP, is also in accordance with the aggressive infiltrative properties of the disease and its association with poor prognostic outcomes for patients.[50,51]

Combined assessment of Appl1, Sortilin and Syndecan-1 showed similar labelling for IDCP and invasive prostatic adenocarcinoma, providing evidence for the retrograde spread theory for IDCP. Interestingly, cribriform IDCP displays a strong Appl1, Sortilin and Syndecan-1 labelling pattern, compared with minimal Sortilin labelling in solid IDCP architectural patterns. These data align with our recent findings, suggesting that reduced expression of Sortilin is indicative of aggressive high-grade forms of prostate cancer (consisting of poorly formed glands, sheets/nests of cells and/or carcinoma with comedonecrosis).[20] Most IDCP is associated with high-grade prostatic adenocarcinoma, suggesting that IDCP is a retrograde extension of invasive cancer into ducts and acini.[18,19] It has recently become apparent that IDCP and invasive prostatic adenocarcinoma share clonal ancestry; for example, IDCP can be derived from adjacent PTEN-negative prostatic adenocarcinoma, with an identical TMPRSS2-ERG breakpoint.[18,19] Very few cases of isolated IDCP which are unaccompanied by invasive cancer have been reported, and it has been suggested that in rare cases IDCP might represent a precancerous lesion.[3,52] However, the limited number of cases that have been reported does suggest that rather than being an *in situ* lesion, this is more likely representative of cases where the primary cancer has not been detected in the tissue sections. In this series of patients, all cases of IDCP were associated with invasive prostatic adenocarcinoma. The biomarker panel, Appl1, Sortilin and Syndecan-1, displayed similar labelling patterns between IDCP and adjacent invasive prostatic adenocarcinoma, and cancer with the most aggressive phenotype was evident in the prostatic ducts and acini. Thus, these data provide evidence supporting the theory of retrograde spread for invasive high-grade prostate cancer into ducts and acini in a manner somewhat similar to perineural and microvascular invasion by the tumour; and indeed, the latter pathologies were evident in this series of patient samples. This similarity of biomarker expression in IDCP and surrounding tissue adds weight to the argument that the grading of IDCP should be included in the five-tier Gleason grading system.[8]

In conclusion, the novel IHC panel of Appl1, Sortilin and Syndecan-1 showed concordance between IDCP and adjacent cancer, providing additional evidence supporting the retrograde spread of invasive prostatic adenocarcinoma into pre-existing ducts and acini. This similar pattern of biomarker expression in IDCP and surrounding adenocarcinoma tissue also supports the inclusion of IDCP grading into the final Gleason grade which, in turn, should promote standardisation of patient reporting and management.

APPENDIX A. SUPPLEMENTARY DATA

Supplementary data related to this article can be found at https://doi.org/10.1016/j.pathol.2023.05.004.

Address for correspondence: Dr Carmela Martini, University of South Australia, Bradley Building, City West Campus, North Terrace, Adelaide, SA 5000, Australia. E-mail: carmela.martino@unisa.edu.au

References

1. Sung H, Ferlay J, Siegel RL, *et al*. Global Cancer Statistics 2020: GLOBOCAN estimates of incidence and mortality worldwide for 36 cancers in 185 countries. *CA Cancer J Clin* 2021; 71: 209−49.
2. Watts K, Li J, Magi-Galluzzi C, *et al*. Incidence and clinicopathological characteristics of intraductal carcinoma detected in prostate biopsies: a prospective cohort study. *Histopathology* 2013; 63: 574−9.
3. Grypari IM, Logotheti S, Lazaris AC, *et al*. Isolated intraductal carcinoma of the prostate in prostatectomy specimens: report of 2 cases and review of the literature. *Int J Surg Pathol* 2020; 28: 918−24.
4. Porter LH, Lawrence MG, Ilic D, *et al*. Systematic review links the prevalence of intraductal carcinoma of the prostate to prostate cancer risk categories. *Eur Urol* 2017; 72: 492−5.
5. Cohen RJ, Chan WC, Edgar SG, *et al*. Prediction of pathological stage and clinical outcome in prostate cancer: an improved pre-operative model incorporating biopsy-determined intraductal carcinoma. *Br J Urol* 1998; 81: 413−8.
6. Kimura K, Tsuzuki T, Kato M, *et al*. Prognostic value of intraductal carcinoma of the prostate in radical prostatectomy specimens. *Prostate* 2014; 74: 680−7.
7. Epstein JI, Amin MB, Fine SW, *et al*. The 2019 Genitourinary Pathology Society (GUPS) white paper on contemporary grading of prostate cancer. *Arch Pathol Lab Med* 2021; 145: 461−93.
8. van Leenders G, van der Kwast TH, Grignon DJ, *et al*. The 2019 International Society of Urological Pathology (ISUP) consensus conference on grading of prostatic carcinoma. *Am J Surg Pathol* 2020; 44: e87−99.
9. Seipel AH, Delahunt B, Samaratunga H, *et al*. Diagnostic criteria for ductal adenocarcinoma of the prostate: interobserver variability among 20 expert uropathologists. *Histopathology* 2014; 65: 216−27.
10. Humphrey PA, Moch H, Cubilla AL, *et al*. The 2016 WHO Classification of Tumours of the Urinary System and Male Genital Organs-Part B: Prostate and Bladder Tumours. *Eur Urol* 2016; 70: 106−19.
11. Varma M, Epstein JI. Head to head: should the intraductal component of invasive prostate cancer be graded? *Histopathology* 2021; 78: 231−9.
12. Guo CC, Epstein JI. Intraductal carcinoma of the prostate on needle biopsy: histologic features and clinical significance. *Mod Pathol* 2006; 19: 1528−35.

13. Epstein JI, Egevad L, Amin MB, *et al*. The 2014 International Society of Urological Pathology (ISUP) consensus conference on Gleason grading of prostatic carcinoma: definition of grading patterns and proposal for a new grading system. *Am J Surg Pathol* 2016; 40: 244−52.
14. Fine SW, Al-Ahmadie HA, Chen YB, *et al*. Comedonecrosis revisited: strong association with intraductal carcinoma of the prostate. *Am J Surg Pathol* 2018; 42: 1036−41.
15. Lotan TL, Gumuskaya B, Rahimi H, *et al*. Cytoplasmic PTEN protein loss distinguishes intraductal carcinoma of the prostate from high-grade prostatic intraepithelial neoplasia. *Mod Pathol* 2013; 26: 587−603.
16. Morais CL, Han JS, Gordetsky J, *et al*. Utility of PTEN and ERG immunostaining for distinguishing high-grade PIN from intraductal carcinoma of the prostate on needle biopsy. *Am J Surg Pathol* 2015; 39: 169−78.
17. Khani F, Wobker SE, Hicks JL, *et al*. Intraductal carcinoma of the prostate in the absence of high-grade invasive carcinoma represents a molecularly distinct type of in situ carcinoma enriched with oncogenic driver mutations. *J Pathol* 2019; 249: 79−89.
18. Taylor RA, Fraser M, Livingstone J, *et al*. Germline BRCA2 mutations drive prostate cancers with distinct evolutionary trajectories. *Nat Commun* 2017; 8: 13671.
19. Haffner MC, Weier C, Xu MM, *et al*. Molecular evidence that invasive adenocarcinoma can mimic prostatic intraepithelial neoplasia (PIN) and intraductal carcinoma through retrograde glandular colonization. *J Pathol* 2016; 238: 31−41.
20. Martini C, Logan JM, Sorvina A, *et al*. Aberrant protein expression of Appl1, Sortilin and Syndecan-1 during the biological progression of prostate cancer. *Pathology* 2023; 55: 40−51.
21. Johnson IR, Parkinson-Lawrence EJ, Butler LM, *et al*. Prostate cell lines as models for biomarker discovery: performance of current markers and the search for new biomarkers. *Prostate* 2014; 74: 547−60.
22. Johnson IR, Parkinson-Lawrence EJ, Shandala T, *et al*. Altered endosome biogenesis in prostate cancer has biomarker potential. *Mol Cancer Res* 2014; 12: 1851−62.
23. Johnson IRD, Parkinson-Lawrence EJ, Keegan H, *et al*. Endosomal gene expression: a new indicator for prostate cancer patient prognosis? *Oncotarget* 2015; 6: 37919−29.
24. Logan JM, Hopkins AM, Martini C, *et al*. Prediction of Prostate Cancer Biochemical and Clinical Recurrence Is Improved by IHC-Assisted Grading Using Appl1, Sortilin and Syndecan-1. *Cancers (Basel)* 2023; 15: 3215.
25. Diggins NL, Webb DJ. APPL1 is a multifunctional endosomal signaling adaptor protein. *Biochem Soc Trans* 2017; 45: 771−9.
26. Wang S, Zhang X, Wang G, *et al*. Syndecan-1 suppresses cell growth and migration via blocking JAK1/STAT3 and Ras/Raf/MEK/ERK pathways in human colorectal carcinoma cells. *BMC Cancer* 2019; 19: 1160.
27. Tanimoto R, Morcavallo A, Terracciano M, *et al*. Sortilin regulates progranulin action in castration-resistant prostate cancer cells. *Endocrinology* 2015; 156: 58−70.
28. Blondeau N, Beraud-Dufour S, Lebrun P, *et al*. Sortilin in glucose homeostasis: from accessory protein to key player? *Front Pharmacol* 2018; 9: 1561.
29. Samaratunga H, Delahunt B, Yaxley JW, *et al*. Intraductal carcinoma of the prostate: extreme nuclear size is not a diagnostic parameter. *Am J Surg Pathol* 2021; 45: 1527−33.
30. Epstein JI, Allsbrook Jr WC, Amin MB, *et al*. The 2005 International Society of Urological Pathology (ISUP) consensus conference on Gleason grading of prostatic carcinoma. *Am J Surg Pathol* 2005; 29: 1228−42.
31. Woods AE, Ellis RC. *Laboratory Histopathology: A Complete Reference*. Churchill Livingstone, 1994. −6.
32. Rathod SG, Jaiswal DG, Bindu RS. Diagnostic utility of triple antibody (AMACR, HMWCK and P63) stain in prostate neoplasm. *J Fam Med Prim Care* 2019; 8: 2651−5.
33. Varma M, Delahunt B, Egevad L, *et al*. Intraductal carcinoma of the prostate: a critical re-appraisal. *Virchows Arch* 2019; 474: 525−34.
34. Song J, Mu Y, Li C, *et al*. APPL proteins promote TGFβ-induced nuclear transport of the TGFβ type I receptor intracellular domain. *Oncotarget* 2016; 7: 279−92.
35. Bogan JS, Kandror KV. Biogenesis and regulation of insulin-responsive vesicles containing GLUT4. *Curr Opin Cell Biol* 2010; 22: 506−12.
36. Pan X, Zaarur N, Singh M, *et al*. Sortilin and retromer mediate retrograde transport of Glut4 in 3T3-L1 adipocytes. *Mol Biol Cell* 2017; 28: 1667−75.
37. Ronen S, Abbott DW, Kravtsov O, *et al*. PTEN loss and p27 loss differ among morphologic patterns of prostate cancer, including cribriform. *Hum Pathol* 2017; 65: 85−91.
38. Asplund A, Ostergren-Lundén G, Camejo G, *et al*. Hypoxia increases macrophage motility, possibly by decreasing the heparan sulfate proteoglycan biosynthesis. *J Leukoc Biol* 2009; 86: 381−8.

39. Chua MLK, Lo W, Pintilie M, *et al*. A prostate cancer "nimbosus": genomic instability and SChLAP1 dysregulation underpin aggression of intraductal and cribriform subpathologies. *Eur Urol* 2017; 72: 665−74.
40. Milosevic M, Warde P, Ménard C, *et al*. Tumor hypoxia predicts biochemical failure following radiotherapy for clinically localized prostate cancer. *Clin Cancer Res* 2012; 18: 2108−14.
41. Bhandari V, Hoey C, Liu LY, *et al*. Molecular landmarks of tumor hypoxia across cancer types. *Nat Genet* 2019; 51: 308−18.
42. Kawashima KI, Ishiuchi Y, Konnai M, *et al*. Glucose deprivation regulates the progranulin-sortilin axis in PC12 cells. *FEBS Open Bio* 2017; 7: 149−59.
43. Piscopo P, Rivabene R, Adduci A, *et al*. Hypoxia induces up-regulation of progranulin in neuroblastoma cell lines. *Neurochem Int* 2010; 57: 893−8.
44. Tanimoto R, Palladino C, Xu SQ, *et al*. The perlecan-interacting growth factor progranulin regulates ubiquitination, sorting, and lysosomal degradation of sortilin. *Matrix Biol* 2017; 64: 27−39.
45. Townley RA, Boeve BF, Benarroch EE. Progranulin: functions and neurologic correlations. *Neurology* 2018; 90: 118−25.

46. Porter LH, Hashimoto K, Lawrence MG, *et al*. Intraductal carcinoma of the prostate can evade androgen deprivation, with emergence of castrate-tolerant cells. *BJU Int* 2018; 121: 971−8.
47. Destouni M, Lazaris AC, Tzelepi V. Cribriform patterned lesions in the prostate gland with emphasis on differential diagnosis and clinical significance. *Cancers (Basel)* 2022; 14: 3041.
48. Monami G, Emiliozzi V, Bitto A, *et al*. Proepithelin regulates prostate cancer cell biology by promoting cell growth, migration, and anchorage-independent growth. *Am J Pathol* 2009; 174: 1037−47.
49. O'Sullivan MJ, Lindsay AJ. The endosomal recycling pathway - at the crossroads of the cell. *Int J Mol Sci* 2020; 21: 6074.
50. Tsuzuki T. Intraductal carcinoma of the prostate: a comprehensive and updated review. *Int J Urol* 2015; 22: 140−5.
51. Zhou M. Intraductal carcinoma of the prostate: the whole story. *Pathology* 2013; 45: 533−9.
52. Robinson BD, Epstein JI. Intraductal carcinoma of the prostate without invasive carcinoma on needle biopsy: emphasis on radical prostatectomy findings. *J Urol* 2010; 184: 1328−33.